



Published in final edited form as:

Proc SPIE Int Soc Opt Eng. 2013 March 12; 8671: 867117-. doi:10.1117/12.2007669.

A Fully Actuated Robotic Assistant for MRI-Guided Prostate Biopsy and Brachytherapy

Gang Li^{a,*}, Hao Su^a, Weijian Shang^a, Junichi Tokuda^b, Nobuhiko Hata^b, Clare M. Tempany^b, and Gregory S. Fischer^a

^aDepartment of Mechanical Engineering, Worcester Polytechnic Institute, Worcester, MA, USA

^bDepartment of Radiology, Brigham and Women's Hospital, Boston, MA, USA

Abstract

Intra-operative medical imaging enables incorporation of human experience and intelligence in a controlled, closed-loop fashion. Magnetic resonance imaging (MRI) is an ideal modality for surgical guidance of diagnostic and therapeutic procedures, with its ability to perform high resolution, real-time, high soft tissue contrast imaging without ionizing radiation. However, for most current image-guided approaches only static pre-operative images are accessible for guidance, which are unable to provide updated information during a surgical procedure. The high magnetic field, electrical interference, and limited access of closed-bore MRI render great challenges to developing robotic systems that can perform inside a diagnostic high-field MRI while obtaining interactively updated MR images. To overcome these limitations, we are developing a piezoelectrically actuated robotic assistant for actuated percutaneous prostate interventions under real-time MRI guidance. Utilizing a modular design, the system enables coherent and straight forward workflow for various percutaneous interventions, including prostate biopsy sampling and brachytherapy seed placement, using various needle driver configurations. The unified workflow comprises: 1) system hardware and software initialization, 2) fiducial frame registration, 3) target selection and motion planning, 4) moving to the target and performing the intervention (e.g. taking a biopsy sample) under live imaging, and 5) visualization and verification. Phantom experiments of prostate biopsy and brachytherapy were executed under MRI-guidance to evaluate the feasibility of the workflow. The robot successfully performed fully actuated biopsy sampling and delivery of simulated brachytherapy seeds under live MR imaging, as well as precise delivery of a prostate brachytherapy seed distribution with an RMS accuracy of 0.98mm.

Keywords

Magnetic resonance imaging; image-guided intervention; MRI-compatible robot; prostate biopsy; prostate brachytherapy; piezoelectric actuation; automated needle insertion

*{gli2, gfischer}@wpi.edu; phone 1-508-831-5191; <http://aimlab.wpi.edu>.

1. INTRODUCTION

Needle-based percutaneous interventions include biopsy, which is the gold standard for diagnosis, and brachytherapy, which is a common treatment for prostate cancer. Image-guided therapy (IGT) affords higher precision and greater outcomes for interventional procedure, by providing intuitive anatomic structure of the tissue. Magnetic resonance imaging is an ideal guidance tool for IGT due to its ability to perform high quality, real-time, volumetric imaging without ionizing radiation. Robotic assistance enables high accuracy and reliability surgical procedures, and can streamline the clinical workflow. Image-guided interventional robotic systems have been investigated with considerable efforts during the last decades. Krieger et al. presented a 2 degree-of-freedom (DOF) passive and manually manipulated robot to perform transrectal prostate biopsy under MRI-guidance^[1]. Fischer et al.^[2] designed a pneumatically actuated robotic system for prostate biopsy and intervention, and further refined by Song et al, replacing the 2-DOF Cartesian motion with a 4 DOF parallel platform enabling needle angulation^[3]. Stoianovici et al. presented an MRI-guided automatic brachytherapy seed placement robot based on pneumatic actuation^[4]. Yu et al. designed a 16 DOF robotic system for prostate brachytherapy with ultrasound probe^[5]. Fichtinger et al. developed a couch-mounted system for prostate biopsy and therapy with intraoperative computed tomography (CT) guidance^[6]. However, manual needle insertion is adopted by most current image-guided approaches, because it is comparatively easy and inherently safe to implement, without the requirement of actuation and high precision coordinated motion control. Automated needle insertion could provide significant advantages over manual insertion with respect to time consumption, repeatability and ergonomics. With an automated needle insertion, clinicians can control the robot from outside the tightly constrained scanner bore, reducing the time consumed on manual alignment or insertion, decreasing the error introduced by clinician's physiological tremor, and avoiding uncomfortable or fatigable posture during the procedure. It also offers the potential of tele-operated needle placement, which could further improve the workflow by including the human in the loop, while maintaining the ability to perform intra-operative MR imaging. Traditional methods typically rely on pre-operative images, which could not reflect the updated information during the surgical procedure. Intra-operative imaging enables closed-loop medicine, by offering real-time vision feedback.

This study focuses on developing and validating an MRI-compatible piezoelectrically actuated robotic system for automated prostate interventions. This system enables a straightforward and coherent workflow for prostate biopsy, brachytherapy and most other standard needle placement procedures.

2. METHODS

2.1 System Architecture

A modular design approach is utilized to develop the system, supporting many typical needle-based percutaneous interventions. This system comprises four major modules: 1) MRI visualization and navigation software, 2) robot control interface software, 3) MRI robot controller, and 4) the interventional robot. The open-source image navigation software 3D Slicer^[5] is used to select and visualize targets in the image space. The system workflow is

organized by the robot control software, which is connected to the navigation software via OpenIGTLink communication protocol^[5]. Non-harmonic piezoelectric motors (PiezoMotor actuators, Uppsala, Sweden) are selected as the actuators, for the better accuracy, dynamic performance and robustness comparing with the pneumatic actuators, and for better noise suppression comparing with harmonic piezoelectric counterparts. The custom MRI robot controller resides in the scanner room and provides high precision closed-loop control of the piezoelectric motors^[10]. Fiber optic Ethernet, running through the patch panel of MRI scanner room, establishes the connection between the robot control software (running on a computer in the console room) and robot controller (beside the MRI scanner), to eliminate the transmission of any electrical signals into the scanner room that may introduce noise into the imaging. The desired target position selected in the 3D Slicer navigation software is sent to the robot control software, wherein it is resolved to the motion commands of individual joints through inverse kinematics that take into account the robot registration, and then interpreted by the robot controller to drive individual motors and move the robot to the desired position. The actual needle position is sent back to the 3D Slicer in patient coordinates for verification and visualization through forward kinematics running in the robot control software. Fig. 1 (left) illustrates the configuration of the system distinguishing the components inside the scanner room and in the console room. The the system architecture and data flow is shown in Fig. 1 (right).

2.2 System Workflow

The workflow of the system mimics that of traditional template-based transperineal prostate interventions guided by transrectal ultrasound (TRUS), as shown in Fig. 2. By utilizing a modular robot design, the system could implement biopsy, brachytherapy and most other standard needle-based prostate interventions with only minor modifications of the workflow. The unified workflow consists of five major steps:

1. **Initialization:** Initialize the hardware and software of system. Initialize all the robot joints and move the robot to the defined home position.
2. **Registration:** Capture a small MR image volume of the fiducial frame. Perform fiducial frame registration, using multi-image registration method^[9].
3. **Planning:** Capture MR images of the prostate and define targets in the MR images via navigation software. Transmit the targets to robot control software over OpenIGTLink for processing inverse kinematics and solving joint space commands.
4. **Targeting:** Move the robot to the desired target position and perform corresponding clinical procedure under live image guidance. The targeting procedure could be modified to implement various interventions according to specific clinical procedures, including image-guided biopsy, brachytherapy, and others requiring straight needle insertion.
5. **Verification:** Visualize the reported actual needle position and interactively updated images in the navigation software for verification.

2.3 Prostate Intervention Robot

The robot mechanism is designed to perform robot-assisted biopsy and brachytherapy with actuated insertion directly under the clinician's control. The 6 DOF robot consists of a 3 DOF Cartesian stage and a 3 DOF needle driver module, as shown in Fig. 3. The needle driver offers 1 DOF cannula translation, 1 DOF stylet translation, and 1 DOF cannula rotation that can be used to potentially reduce the needle insertion force and needle deflection. Coordinated motion can be implemented between the cannula translation and stylet translation under high precision motion control, to perform fully actuated biopsy sampling and brachytherapy seed placement smoothly and precisely. The universal needle clamping mechanism is developed to fasten varying sizes of standard needles, from 25 Gauge (0.5144mm) to 16 Gauge (1.651mm), by using the corresponding collet. The design allows a variety of needles to be mounted on the needle driver by choosing specific needle adaptors, including those for various biopsy needles, brachytherapy needles and other needles and cannulas.

To register the robot to the RAS (Right, Anterior, Superior) patient coordinate system in the image space, a fiducial frame is firmly attached to the base of the robot as shown in Fig. 3. The fiducial frame is composed of seven tubes filled with MR-visible, high contrast fluid (Beekley, Bristol, CT), and configured in a set of Z shapes in each of the three orthogonal planes^[9]. Based on imaging the fiducial frame, the 6 DOF position and orientation of the robot can be localized with respect to the RAS patient coordinates.

3. EXPERIMENTS AND RESULTS

To evaluate the feasibility of the system workflow and the flexibility of the modular design approach, phantom experiments of automated prostate biopsy and brachytherapy were performed under MRI-guidance. The experimental setup utilized in a 3T MRI scanner is shown in Fig. 4. Gelatin phantoms used in these tests are firmer than the regular tissue to avoid the gelatin to deflect during needle insertion.

3.1 Biopsy Experiment

Beans with an approximate diameter of 9mm, which is similar to the size of a tumor to be targeted, were embedded in a gelatin phantom to serve as biopsy targets. An 18G MRI biopsy needle is placed in the gelatin phantom by the robot and imaged with real-time imaging protocol during the intervention. The procedure for executing a biopsy is shown in Fig. 5. According to this procedure, we can specify the clinical targeting procedure in the unified workflow as depicted in Section 2.2:

1. Align the robot to the plane of the entry point.
2. Insert the cannula to the depth of L before the target position, guaranteeing the sample at the center of notch. (L equals to the distance from the tip of stylet to the notch center.)
3. Sample biopsy under automatic procedure. Insert stylet distance of $2L$, making the notch center at target sample position. Perform coordinated motion to insert

cannula and retract stylet with the same length $2L$ and under the same speed to capture the sample inside the needle.

4. Retract needle containing the biopsy core to home position.

3.2 Brachytherapy Experiment

To evaluate capabilities for brachytherapy, a 3×3 pattern of needles with three seeds per needles was applied with the robot. Custom made brass seeds and plastic spacers are employed to mimic the radioactive seeds, with length of 5mm for both seed and spacer. The seeds and spacers could be distinguished under MRI images with their different imaging properties, i.e. introducing different artifacts. An 18G MRI brachytherapy needle is placed in the gelatin phantom and imaged with T2-weighted fast spin echo imaging protocol (T2W TSE). The procedure for executing brachytherapy is shown in Fig. 7 and can be specified the in the unified workflow:

1. Retract stylet joint to depth L , and load the seeds and spacers to the brachytherapy needle according to the treatment plan. (L equals to the sum of the length of the seeds and the spacers). Alternatively, pre-loaded needles may be loaded into the needle driver.
2. Align the robot such that the needle axis is in line with the planned entry point.
3. Insert the cannula along the needle axis to the target position.
4. Deliver seeds under automatically coordinated motion, retracting cannula and inserting stylet with the same length L and under the same speed.
5. Retract needle to home position.

Both MRI and CT images were utilized to analyze the experimental results. MRI image was used demonstrate feasibility and qualitatively to illustrate the pattern of the seeds and spacers, as shown in Fig. 8. Due to its very high resolution, CT images were used for quantitative analysis of the seed placement distribution. The proposed seeds distribution pattern was compared with the actual pattern (as measured using the segmented high resolution CT scan of the phantom with implanted seeds, as shown in Fig. 8). A point cloud registration between the plan and the segmented CT was used to determine the accuracy of the seeds placement pattern; absolute location with respect to the scanner was not assessed. The experimental results demonstrate submillimeter accuracy of the seed distribution, with an RMS error of approximately 0.98mm and a standard deviation of approximately 0.37mm. The error in seed placement may be due to needle deflection, considering the bevel tip of the brachytherapy needle, which could be reduced by rotating the cannula to reduce the insertion force. The custom made seeds and spacers are not exactly the same length, that could also introduce some errors.

4. CONCLUSION

This paper presents a fully actuated approach to transperineal MRI-guided prostate biopsy and brachytherapy using a piezoelectrically actuated robotic system. Phantom experiments validate the capability and flexibility of the system to execute automated prostate biopsy and

brachytherapy with only minor modification of the typical clinical workflow. The preliminary results are satisfactory with an RMS seeds placement accuracy of approximately 0.98mm. MRI compatibility of the system showing no significant image quality degradation during robot motion has been demonstrated in other studies^[12]. The proposed architecture overcomes many of the limitations of manual insertion (fully manual or robot-assisted alignment) by allowing the clinician to control the robot from beside the patient but outside the tightly constrained bore. The MRI-guided automated needle placement robotic system provides some significant advantages over manual approaches, including 1) improved work flow: the work flow is more straightforward and coherent, with the robot assistance and high resolution image guidance, 2) increased position accuracy, the individual robot joint accuracy could be as high as 30 μm ^[11], and 3) reduced time consumption, especially for multiple needle insertions: biopsy and brachytherapy procedures are executed automatically, under coordinated motion.

In the future work, teleoperation with force feedback will be integrated with the system, which enables human experience and intelligence to be included in the control loop such that the needle depth may be teleoperated while observing real-time images, and will further improve the surgical workflow, safety and quality.

ACKNOWLEDGEMENTS

This work is supported in part by the Congressionally Directed Medical Research Programs Prostate Cancer Research Program (CDMRP PCR) New Investigator Award W81XWH-09-1-0191, the American Society of Quality Schlesinger Award, and NIH awards 5P41RR019703, 5P01CA067165, 1R01CA111288.

REFERENCES

- [1]. Krieger A, Iordachita II, Guion P, Singh AK, Kaushal A, Menard C, Pinto PA, Camphausen K, Fitchinger G, Whitcomb LL. An MRI-compatible robotic system with hybrid tracking for MRI-guided prostate intervention. *Transactions on Biomedical Engineering*. 2011; 58(11):3049–3061.
- [2]. Fischer GS, Iordachita II, Csoma C, Tokuda J, DiMaio SP, Tempany CM, Hata N, Fitchinger G. MRI-compatible pneumatic robot for transperineal prostate needle placement. *Transactions on Mechatronics*. 2008; 13(3):295–305. [PubMed: 21057608]
- [3]. Song, S-E.; Cho, NB.; Fischer, GS.; Hata, N.; Tempany, CM.; Fitchinger, G.; Iordachita, II. Development of a pneumatic robot for MRI-guided transperineal prostate biopsy and brachytherapy: new approaches. *IEEE International Conference on Robotics and Automation*; 2010. p. 2580-2586.
- [4]. Patriciu A, Petrisor D, Muntener M, Mazilu D, Schär M, Stoianovici D. Automatic brachytherapy seed placement under MRI guidance. *Transactions on Biomedical Engineering*. 2007; 54(8): 1499–1506.
- [5]. Yu Y, Podder T, Zhang Y, Ng W, Mistic V, Sherman J, Fu L, Fuller D, Messing E, Rubens D, Strang J, Brasacchio R. Robot-assisted Prostate Brachytherapy. *Medical Image Computing and Computer-Assisted Intervention*. 2006:41–49. [PubMed: 17354872]
- [6]. Fichtinger G, DeWeese TL, Patriciu A, Tanacs A, Mazilu D, Anderson JH, Masamune K, Taylor RH, Stoianovici D. System for robotically assisted prostate biopsy and therapy with intraoperative CT guidance. *Academic Radiology*. 2002; 9(1):60–74. [PubMed: 11918360]
- [7]. Gering DT, Nabavi A, Kikinis R, Hata N, O'Donnell LJ, Grimson WE, Jolesz FA, Black PM, Wells WM. An integrated visualization system for surgical planning and guidance using image fusion and an open MR. *J Magn Reson Imag*. 2001; 13(6):967–975.
- [8]. Tokuda J, Fischer GS, Papademetris X, Yaniv Z, Ibanez L, Cheng P, Liu H, Blevins J, Arata J, Golby AJ, Kapur T, Pieper S, Burdette EC, Fichtinger G, Tempany CM, Hata N. *OpenIGTLink*:

an open network protocol for image-guided therapy environment. *Int J Med Robot.* 2009; 5(4): 423–434. [PubMed: 19621334]

- [9]. Shang W, Fischer GS. A high accuracy multi-image registration method for tracking MRI-guided robots. *Proc. SPIE.* 2012; 8316:83161V–83161V-8.
- [10]. Su, H.; Cardona, DC.; Shang, W.; Camilo, A.; Cole, GA.; Rucker, DC.; Webster, RJ.; Fischer, GS. A MRI-guided concentric tube continuum robot with piezoelectric actuation: a feasibility study. *International Conference on Robotics and Automation*; 2012. p. 1939-1945.
- [11]. Su H, Shang W, Harrington K, Camilo A, Cole G, Tokuda J, Hata N, Tempany C, Fischer GS. A Networked Modular Hardware and Software System for MRI-guided Robotic Prostate Interventions. *Proc. SPIE.* 2012; 8316:83161Z–83161Z-8.
- [12]. Su, H.; Zervas, M.; Cole, GA.; Furlong, C.; Fischer, GS. Real-time MRI-guided needle placement robot with integrated fiber optic force sensing. *International Conference on Robotics and Automation*; 2011. p. 1583-1588.

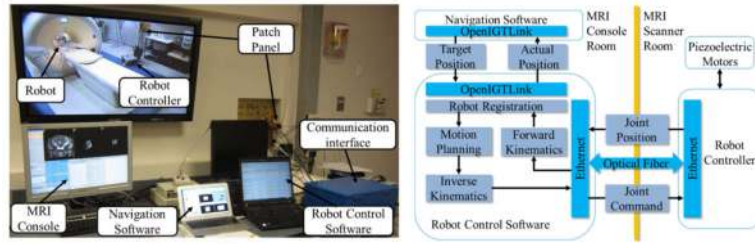


Figure 1. Configuration of the MRI-guided interventional robot in a typical 3T diagnostic MRI scanner (left), with the robot controller inside the scanner room beside the bore and the interface software running on computers in the console room connected through a fiberoptic network. Diagram of system architecture and data flow between the components (right).

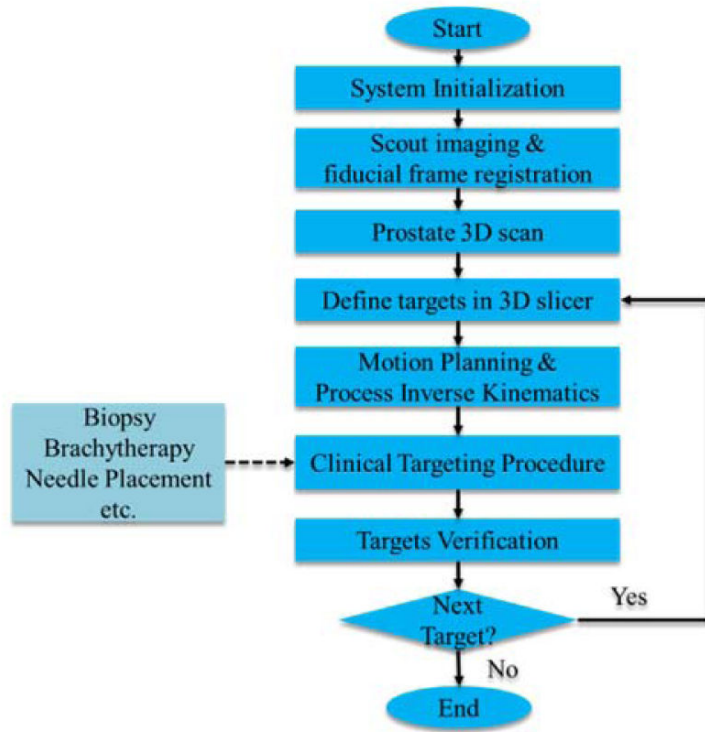


Figure 2. Unified workflow of MRI-guided robot-assisted prostate interventions.

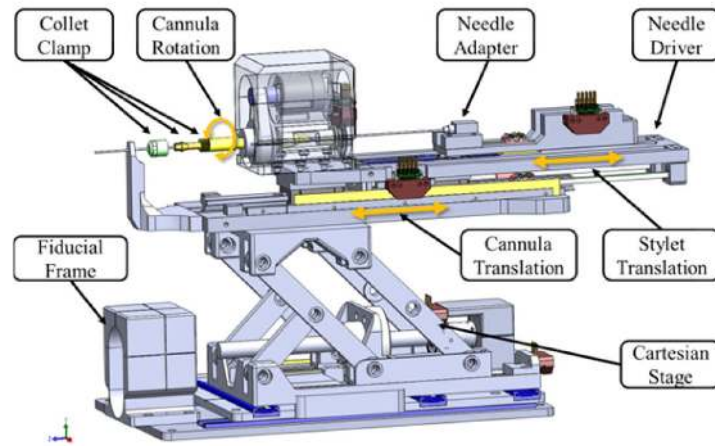


Figure 3. 3D CAD model of the prostate interventional robot showing Cartesian stage, needle driver, and fiducial frame.

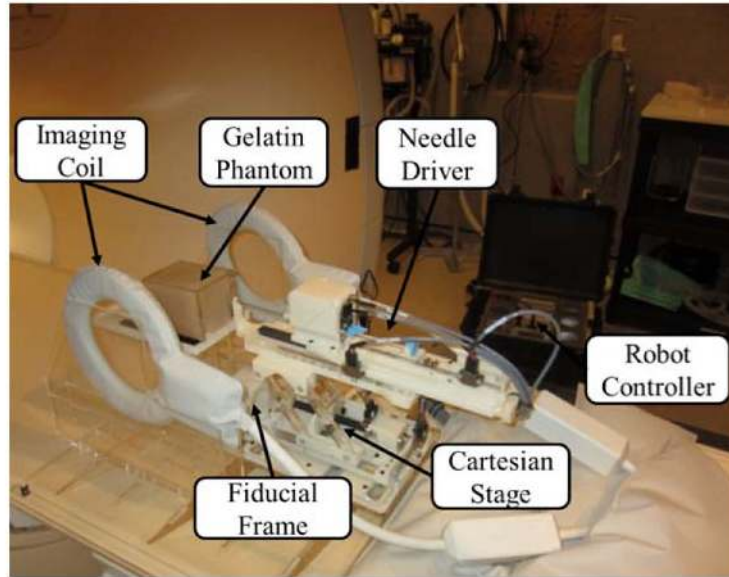


Figure 4.
The prostate interventional robot at the entrance of the bore to a 3T MRI scanner showing the phantom experimental setup.

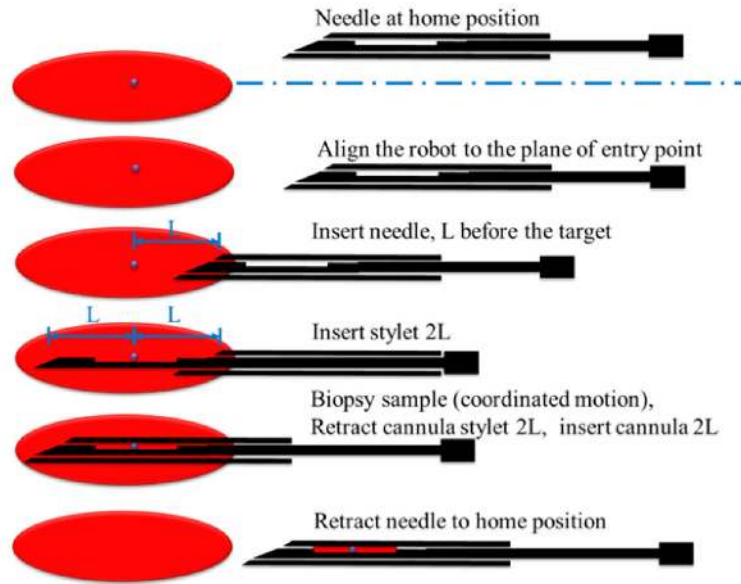


Figure 5.
The clinical procedure for executing automated biopsy.

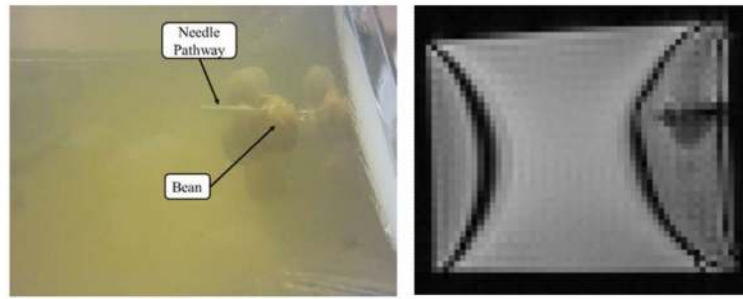


Figure 6. (Left) Gelatin phantom with biopsy targets and (right) real-time MRI image of the target in the gelatin phantom showing the needle in the bean.

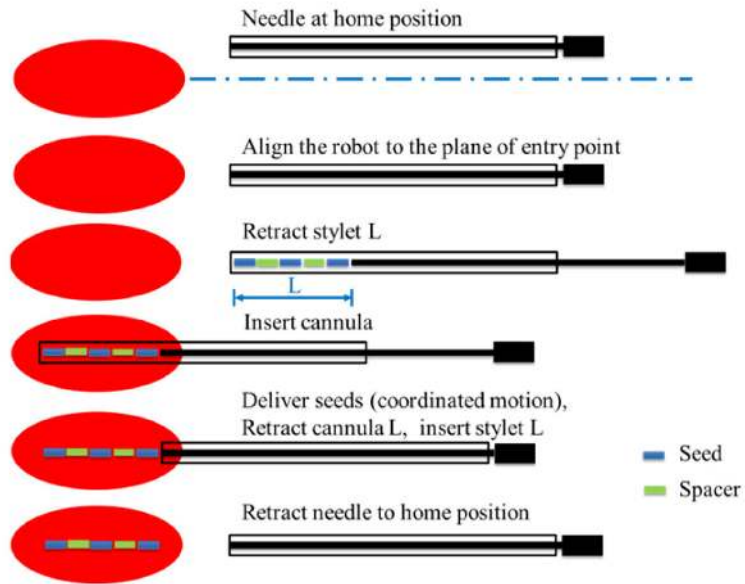


Figure 7. The clinical procedure for executing automated brachytherapy seed delivery.

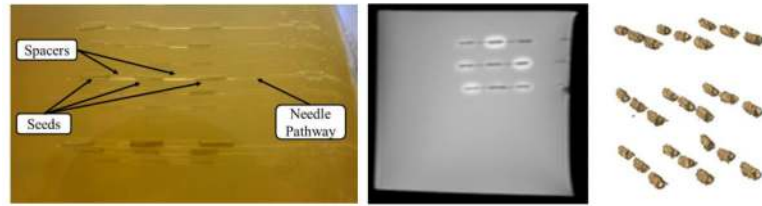


Figure 8. (Left) Gelatin phantom showing the $3 \times 3 \times 3$ robotically placed brachytherapy seeds, (center) a representative MRI showing one plane of seeds, and (right) segmented 3D CT image of the target gelatin phantom used for accuracy assessment.